Hindawi Publishing Corporation
International Journal of Antennas and Propagation
Volume 2012, Article ID 874840, 9 pages
doi:10.1155/2012/874840

Research Article

Asymptotic Modeling of Coherent Scattering from Random Rough Layers: Application to Road Survey by GPR at Nadir

Nicolas Pinel,[1] Cédric Le Bastard,[1,2] Christophe Bourlier,[1] and Meng Sun[3]

[1] *Institut d'Electronique et de Télécommunications de Rennes (IETR) Laboratory, L'Université de Nantes Angers Le Mans (L'UNAM), UMR CNRS 6164, Polytech Nantes, La Chantrerie, Rue C. Pauc, BP 50609, 44306 Nantes Cedex 3, France*
[2] *CETE de l'Ouest, 23 Avenue de l'Amiral Chauvin, BP 69, 49136 Les Ponts de Cé, France*
[3] *South China University of Technology, 381 Wushan Road, Tianhe District, Guangzhou, China*

Correspondence should be addressed to Nicolas Pinel, nicolas.pinel@univ-nantes.fr

Received 15 June 2012; Revised 3 October 2012; Accepted 13 November 2012

Academic Editor: Saba Mudaliar

This paper studies the coherent scattering from random rough layers made up of two uncorrelated random rough surfaces, by considering 2D problems. The results from a rigorous electromagnetic method called PILE (propagation-inside-layer expansion) are used as a reference. Also, two asymptotic analytical approaches are presented and compared to the numerical model for comparison. The cases of surfaces with both Gaussian and exponential correlations are studied. This approach is applied to road survey by GPR at nadir.

1. Introduction

Scattering by random rough surfaces has been the subject of active research from 1960s, in various domains of physics like optics, remote sensing of natural surfaces (sea surfaces, soils, etc.), and so on. Then, this general field of research begins to be rather well known, so that research is now more focused on specific domains like scattering from sea surfaces at high winds (which includes modeling of whitecaps, breaking waves, etc.) or low-grazing angles propagation. Also, the study is generalized to the remote sensing of complex media, for instance by taking volume scattering into account when inhomogeneous media are considered or by dealing with multilayered media.

This paper focuses on the scattering from layered media made up of one or several random rough surfaces and more specifically on the coherent scattering. This can be useful for various applications: in studying indoor propagation at 60 GHz, by taking the roughness of the rendering of office walls into account [1–3], in optics to determine optical constants of films [4] and other applications [5–9], to calculate the grazing incidence forward (i.e., in the specular direction) radar propagation over sea surfaces [10, 11], and so on.

Here, the study is applied to ground penetrating radar (GPR) for nondestructive pavement survey [12, 13] by taking the roughness of the surfaces into account [14]. Two asymptotic approaches are extended to rough layered media: the scalar Kirchhoff-tangent plane approximation (SKA) and the second-order small perturbation method (SPM2), for calculating the coherent scattering contribution. A numerical rigorous method, named PILE (propagation-inside-layer expansion) method [15], is used as a reference to validate these two asymptotic models. The study focuses on 2D problems with the so-called 1D surfaces, for computational ease of the reference numerical method. This approach is applied to rough layers with two slightly rough surfaces (usually called "two-layer media") characterized by either Gaussian or exponential correlation functions. The height probability density function (PDF) is assumed to be Gaussian.

This paper is organized as follows. Section 2 presents the extension of both the SKA and the SPM2 to calculate the coherent fields scattered from random rough layers. Then, Section 3 presents the numerical results for different scenarios and focuses on the application of road survey by GPR at nadir (i.e., normal incidence).

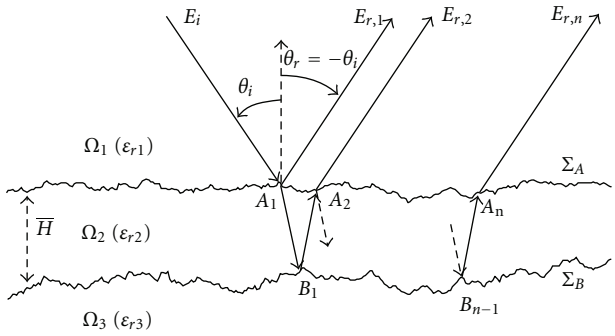

Figure 1: Electromagnetic wave scattering from a 1D random rough layer with two rough surfaces: representation of the first two scattered fields $E_{r,1}$ and $E_{r,2}$.

2. Random Rough Layer Coherent Scattering: Asymptotic Modeling

The problem considers a 1D random rough layer made up of two random rough surfaces separating homogeneous media Ω_1 Ω_2 and Ω_3 (2D problem). An incident plane wave impinges inside Ω_1 upon the upper rough surface Σ_A (see Figure 1). Owing to the two surfaces, multiple scattered fields back into Ω_1 occur: not only the field $E_{r,1}$ scattered by the upper rough surface Σ_A, but also higher order fields resulting from the multiple reflections inside Ω_2: $E_{r,2}$, $E_{r,3}$, and so on.

2.1. Coherent Scattering of Slightly Rough Layers: Extension of the Ament Model. To study the influence of surface roughness on the coherent scattered fields, the Rayleigh roughness parameter Ra, which is well known for the case of reflection from single rough interfaces [16], is used. Considering the reflection onto the upper interface Σ_A, it is usually given by the relation [16, 17]

$$\mathrm{Ra}_{r,1} = k_0 n_1 \sigma_{hA} \cos\theta_i, \tag{1}$$

with $n_1 = 1$ being the refractive index of the incidence medium Ω_1, σ_{hA} the RMS height of the upper surface Σ_A, and θ_i the incidence angle relatively to zenith. Equation (1) corresponds to the Rayleigh roughness parameter associated to the scattered field $E_{r,1}$ (see Figure 1). Then, the coherent scattering is given by the ratio of the amplitude of the mean scattered field $|\langle E_{r,1}\rangle|$ with the amplitude of the incident field $|E_i|$ as

$$\frac{|\langle E_{r,1}\rangle|}{|E_i|} = |r_{12}(\theta_i)|\left\langle e^{j2k_0 n_1 \zeta_A \cos\theta_i}\right\rangle, \tag{2}$$

with r_{12} being the Fresnel reflection coefficient at the upper surface, $\langle\cdots\rangle$ the statistical average operator, and ζ_A the random rough surface heights variations; the term $e^{j2k_0 n_1 \zeta \cos\theta_i}$ assumes $e^{-j\omega t}$ time convention. Then, the coherent field attenuation due to the surface roughness is given by

$$\frac{|\langle E_{r,1}\rangle|}{\left|E_{r,1}^{\mathrm{flat}}\right|} = \left\langle e^{j2k_0 n_1 \zeta_A \cos\theta_i}\right\rangle, \tag{3}$$

with $|E_{r,1}^{\mathrm{flat}}|$ being the scattered field amplitude for the equivalent perfectly flat surface, which is given by $|E_{r,1}^{\mathrm{flat}}| = |r_{12}(\theta_i)|\,|E_i|$. It must be noted that this holds for either 2D or 3D problems. For Gaussian statistics (i.e., for a Gaussian height PDF), the above equation simplifies as

$$\frac{|\langle E_{r,1}\rangle|}{\left|E_{r,1}^{\mathrm{flat}}\right|} = e^{-2\mathrm{Ra}_{r,1}^2}. \tag{4}$$

Recent work [17, 18] made it possible to extend the Rayleigh roughness parameter Ra to the case of reflection from a rough layer made up of two rough surfaces. For a Gaussian process (i.e., for rough surfaces with Gaussian height PDF) and a Gaussian autocorrelation function, a satisfactory agreement was found in [17, 19] between the extended Rayleigh roughness parameters and exact numerical results. Hereafter, the results of this approach are analyzed more thoroughly by studying its frequency behaviour and an extension to the case of surfaces with exponential correlation is tested.

For uncorrelated rough surfaces, the extended Rayleigh roughness parameter $\mathrm{Ra}_{r,2}$ associated to the second-order scattered field $E_{r,2}$ is given for lossless media Ω_1 and Ω_2 by [17, 19]

$$\mathrm{Ra}_{r,2} = \sqrt{2\,(\mathrm{Ra}_{t12})^2 + (\mathrm{Ra}_{r23})^2}, \tag{5}$$

with

$$\mathrm{Ra}_{t12} = k_0 \sigma_{hA} \frac{|n_1 \cos\theta_i - n_2 \cos\theta_m|}{2}, \qquad \mathrm{Ra}_{r23} = k_0 n_2 \sigma_{hB} \cos\theta_m, \tag{6}$$

where n_2 is the refractive index of Ω_2, σ_{hB} is the RMS height of the lower surface Σ_B, and θ_m is the propagation angle inside the inner medium Ω_2.

Then, for Gaussian statistics, the so-called coherent field attenuation associated to $E_{r,2}$ is given by

$$\frac{|\langle E_{r,2}\rangle|}{\left|E_{r,2}^{\mathrm{flat}}\right|} = e^{-2\mathrm{Ra}_{r,2}^2}. \tag{7}$$

This derivation can be extended to any order of reflection from a two-layer medium [11]. As a consequence, for Gaussian statistics, the coherent field attenuation associated to the nth order scattered field $E_{r,n}$ is given by

$$\frac{|\langle E_{r,n}\rangle|}{\left|E_{r,n}^{\mathrm{flat}}\right|} = e^{-2\mathrm{Ra}_{r,n}^2}, \quad n \geq 2, \tag{8}$$

where

$$\mathrm{Ra}_{r,n} = \sqrt{2(\mathrm{Ra}_{t12})^2 + (n-1)(\mathrm{Ra}_{r23})^2 + (n-2)(\mathrm{Ra}_{r21})^2}, \tag{9}$$

with

$$\mathrm{Ra}_{r21} = k_0 n_2 \sigma_{hA} \cos\theta_m. \tag{10}$$

This model is then an extension of the so-called Ament model to random rough layers, and which corresponds to using the scalar Kirchhoff-tangent plane approximation (SKA). It is recalled that the above equations are valid for both 2D and 3D problems.

2.2. Coherent Scattering under an Extended SPM2 Model. It is well known that under the SPM2 (second-order small perturbation method) model, the amplitude attenuation of the coherent scattered field $\langle E_{r,1}\rangle$ is given for 2D problems and for Gaussian statistics by the relation [20]

$$\frac{\left|\langle E_{r,1}\rangle\right|}{\left|E_{r,1}^{\text{flat}}\right|} = 1 - 2k_0^2 n_1^2 \sigma_{hA}^2 \cos^2\theta_i. \tag{11}$$

Comparing the classical SPM2 model with the Ament model (SKA model) for a single rough surface Σ_A, it can be easily seen that the SPM2 model for describing the coherent field attenuation can be written in terms of the Rayleigh roughness parameter $\text{Ra}_{r,1}$ as

$$\frac{\left|\langle E_{r,1}\rangle\right|}{\left|E_{r,1}^{\text{flat}}\right|} = 1 - 2\text{Ra}_{r,1}^2. \tag{12}$$

By comparing (12) with (4), in vacuum ($n_1 = 1$), it can be noted that the SPM2 and SKA models become equivalent when the Rayleigh roughness parameter $\text{Ra}_{r,1} \ll 1$, which occurs for all θ_i if the surface RMS height $\sigma_{hA} \ll \lambda_0/2\pi$, with λ_0 the EM wavelength in vacuum. It also occurs, for instance, for rougher surfaces, as soon as θ_i is large enough ($\theta_i \to \pi/2$). Besides, let us note that the criterion $\text{Ra}_{r,1} \ll 1$ corresponds to the validity domain of the SPM2 model; thus, when the SPM model begins to be invalid, the SKA model is expected to depart from the SPM2 model. Hopefully, we expect the SKA model to be still valid in this region.

Then, at least in the domain where the Ament model (or SKA model) and the SPM2 model are both valid, the SPM2 model for describing the amplitude attenuation of the n coherent scattered fields $\langle E_{r,n}\rangle$ of rough two-layer media can be written as

$$\frac{\left|\langle E_{r,n}\rangle\right|}{\left|E_{r,n}^{\text{flat}}\right|} = 1 - 2\text{Ra}_{r,n}^2. \tag{13}$$

Then, the remark for a single rough interface for comparing the SPM2 and SKA models can be extended to the two-layer case: the SPM2 and SKA models become equivalent when the Rayleigh roughness parameter $\text{Ra}_{r,n} \ll 1$.

In what follows, both asymptotic extended models are compared to a numerical reference method to study their validity domain.

3. Numerical Validation

In order to compute the fields scattered from the rough layer, a numerical method, based on the method of moments (MoM), is used as a reference to validate the above two asymptotic methods for 2D problems. This method, called PILE (propagation-inside-layer expansion) method [15], is a rigorous numerical method that can be speeded up by the acceleration methods [21, 22]. In this study, the PILE method is accelerated by the Forward-Backward method (FB) [23] together with the Spectral Acceleration (FB-SA) [24–26] and denoted by PILE + FB-SA [22].

Contrary to other MoM-based reference numerical methods which generally can calculate only the total scattered field from rough layers $E_{\text{tot}} = \sum_{k=1}^{\infty} E_{r,k} = E_{r,1} + E_{r,2} + \cdots$, the PILE method is able to rigorously compute each scattered field contribution ($E_{r,1}$, $E_{r,2}$, and so on, see Figure 1).

3.1. Application to Pavement Survey by GPR at Nadir. The simulation parameters are chosen to match to the conventional GPR configuration used for pavement survey at traffic speed (e.g., [27]), that is, air-coupled radar configuration at vertical incidence (nadir, $\theta_i = 0$). It is assumed that the scope of probing is limited to the first two layers of the pavement structure, which corresponds to the two rough surfaces represented in Figure 1.

The studied pavement structure is made up of a layer medium Ω_2 of ultra-thin asphalt surfacing (UTAS) of mean thickness $\overline{H} = 20\,\text{mm}$ [28], overlying a rolling band Ω_3 of same general composition (see Figure 1 with $\theta_i = 0$). The two asymptotic methods are compared with the numerical model in a much wider frequency band than in [14] (here, $f \in [0.5\,;\,10.0]\,\text{GHz}$), in order to study the frequency limits of the two asymptotic methods. Also, the influence of the correlation length of the surfaces on the validity of the models is studied. The UTAS and the rolling band are assumed to be equivalent to homogeneous media at normal incidence and at the frequency band under study [13, 29, 30]. Their relative permittivities ϵ_r typically range between 4 and 8 [29, 31], and their conductivities σ between 10^{-3} and $10^{-2}\,\text{S/m}$ [32]. For the simulations, we take $\epsilon_{r2} = 4.5$ and $\epsilon_{r3} = 7$, respectively, and $\sigma_2 = 5 \times 10^{-3}\,\text{S/m}$ and $\sigma_3 = 10^{-2}\,\text{S/m}$, respectively. Then, by considering nondispersive media, the complex relative permittivity $\underline{\epsilon}_r$ can be calculated as [14]

$$\underline{\epsilon}_r = \epsilon_r + j\,\frac{\sigma}{2\pi f \epsilon_0}, \tag{14}$$

with $\epsilon_0 = 10^{-9}/36\pi\,\text{F/m}$ the permittivity inside the vacuum. For instance, for $f = 5\,\text{GHz}$, the complex relative permittivities are $\underline{\epsilon}_{r2} = 4.5 + j0.018$ and $\underline{\epsilon}_{r3} = 7 + j0.036$. The two rough interfaces Σ_A and Σ_B are assumed to have a Gaussian height PDF. About the height autocorrelation function, some studies showed that it is closer to an exponential function than a Gaussian one [33, 34]. Then, it is interesting to look at the influence of the choice of correlation on the accuracy of the asymptotic models. In particular, as the so-called Ament model is based on the scalar Kirchhoff-tangent plane approximation (SKA) which is valid for locally flat surfaces, its performances should degrade for changing from Gaussian correlation to exponential correlation. By contrast, the SPM2 model can deal with nonlocally flat surfaces but is limited to slightly rough surfaces; for random rough layers, this corresponds to the following generalized criterion:

$$\text{Ra}_{r,n} \ll 1. \tag{15}$$

For the upper surface Σ_A, the root mean square (RMS) height σ_{hA} is of the order of 0.6–1 mm, and the correlation length L_{cA} of the order of 5–10 mm [33, 34]. For the lower

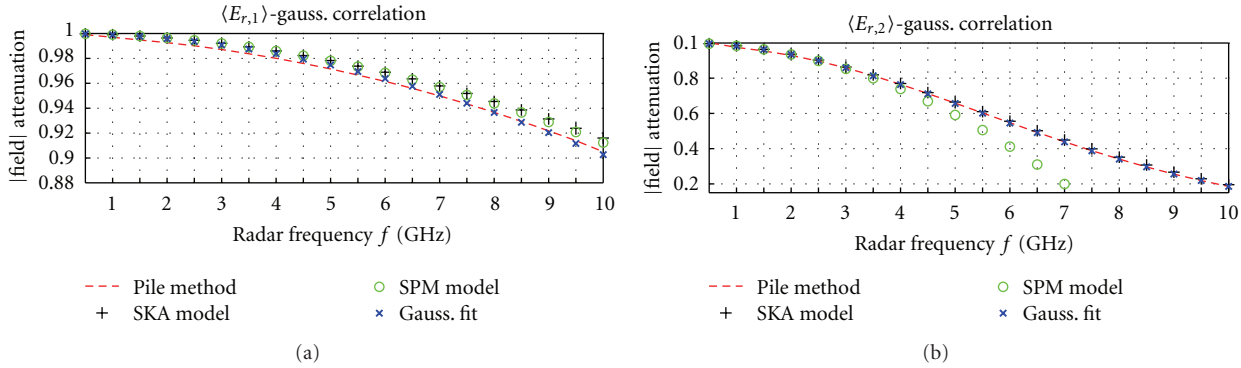

FIGURE 2: Frequency behavior of the amplitude attenuation of the coherent scattered fields $\langle E_{r,1}\rangle$ and $\langle E_{r,2}\rangle$ (V polarization) in the frequency band $f \in [0.5; 10.0]$ GHz, comparatively to the flat case: results from the PILE code and comparison with the SKA and SPM2 asymptotic models for Gaussian surfaces. The upper and lower correlation lengths are $L_{cA} = 10.0$ mm and $L_{cB} = 30.0$ mm, respectively.

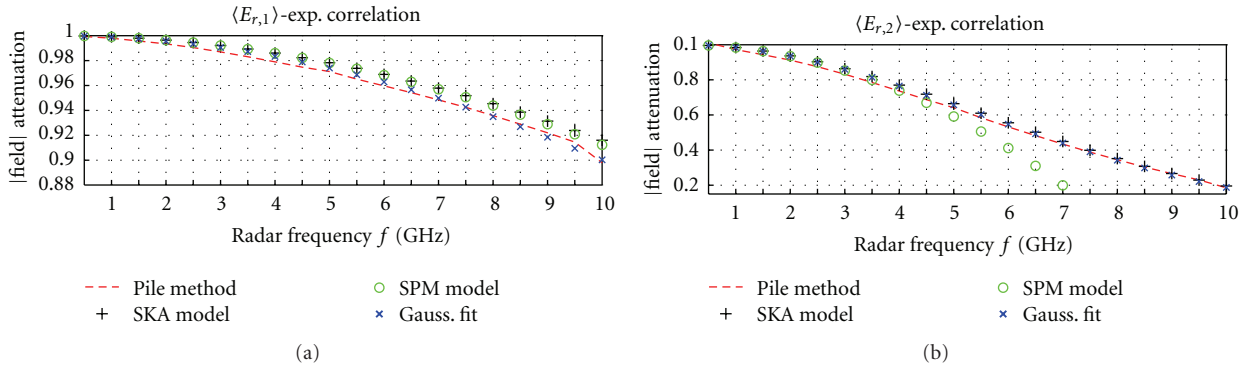

FIGURE 3: The same simulation parameters as in Figure 2 (with $L_{cA} = 10.0$ mm and $L_{cB} = 30.0$ mm), but for exponential correlation surfaces.

surface Σ_B, the RMS height σ_{hB} and the correlation length L_{cB} are a bit greater. For the first scenario to be studied here, chosen simulation parameters are $\sigma_{hA} = 1.0$ mm, $L_{cA} = 10.0$ mm, $\sigma_{hB} = 2.0$ mm, and $L_{cB} = 30.0$ mm. The two rough surfaces are assumed to be uncorrelated [14].

The antenna is assumed to radiate a vertically polarized plane wave in the far field of probed pavement like in [35]: the antenna is about 400 mm above the sand surface, for which the far-field condition has been checked from data. The antenna is thus located beyond the Fraunhofer distance with respect to the probed pavement.

The typical width of probed surface antenna footprint is of the order of 300–500 mm [35, 36]. Then, for the simulations, surfaces of length $L = 2400$ mm are considered, illuminated by a Thorsos beam of attenuation parameter $g = L/6$ [37] (the Thorsos beam is a tapered plane wave, whose tapering has a Gaussian shape; the tapering is used to reduce the incident field to near zero at the ends of the surface realizations and thereby to reduce the edge effects to negligible levels). The two rough interfaces are sampled with a sampling step $\Delta x = \lambda_2/8$, with λ_2 the wavelength inside Ω_2. A normal ($\theta_i = 0$) incident wave is taken, and the first two orders of the reflected fields by the rough layer E_1 and E_2 are calculated by the PILE method at the different frequencies f over the GPR band, that is, $[0.5; 10.0]$ GHz.

3.2. Numerical Results. In Figure 2, the frequency behavior of the amplitude attenuation of $E_{r,1}$ and $E_{r,2}$ in vertical (V) polarization is investigated for Gaussian correlation in the whole range of the band $f \in [0.5; 10]$ GHz, for which $N = 100$ Monte-Carlo processes were used.

As expected, for both contributions, the influence of the roughness of the interfaces continuously increases with frequency, inducing a decrease of the scattered magnitude at nadir. This is confirmed by the Rayleigh roughness parameters $\mathrm{Ra}_{r,1}$ and $\mathrm{Ra}_{r,2}$ which increase as the frequency f increases. The decrease in amplitude is stronger for $\langle E_{r,2}\rangle$ than for $\langle E_{r,1}\rangle$, as predicted by Ra expressions. Moreover, for the first-order $\langle E_{r,1}\rangle$, a general very good agreement of both the SKA and SPM2 models can be found with the PILE reference method. In particular, a perfect match is found for the lower frequencies and for both asymptotic models. Slight differences between the SKA and the SPM2 occur with increasing frequencies, from approximately 8 GHz. For the second-order $\langle E_{r,2}\rangle$, a general excellent agreement of only the SKA model can be found with the PILE reference method. Indeed, the SPM2 model significantly deviates from the PILE method, starting from approximately 3.5–4 GHz. This can be attributed to the fact that $\mathrm{Ra}_{r,2}$ is much higher than $\mathrm{Ra}_{r,1}$; then, the general condition $\mathrm{Ra}_{r,n} \ll 1$ for the SPM2 to be valid occurs for lower frequencies. As a comparison, for

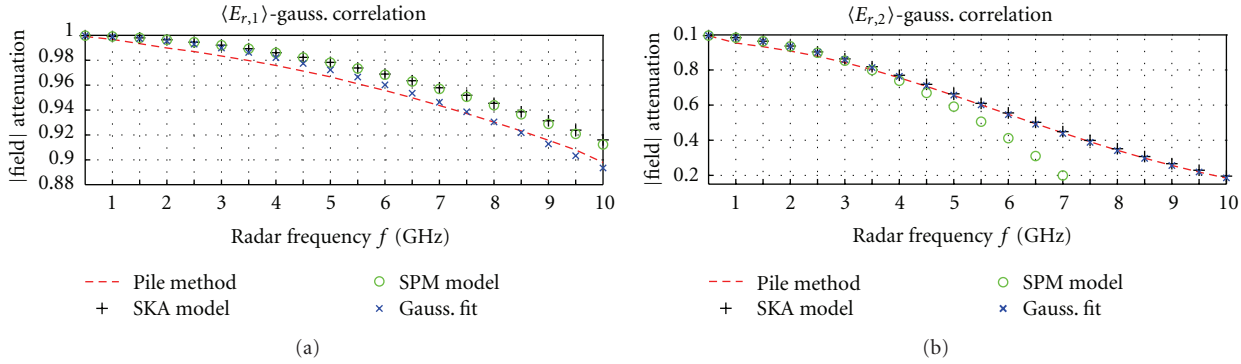

FIGURE 4: Frequency behavior of the amplitude attenuation of the coherent scattered fields $\langle E_{r,1}\rangle$ and $\langle E_{r,2}\rangle$ (V polarization) in the frequency band $f \in [0.5; 10.0]$ GHz, comparatively to the flat case. Results from the PILE code and comparison with the SKA and SPM2 asymptotic models for Gaussian surfaces. The upper and lower correlation lengths are $L_{cA} = 6.4$ mm and $L_{cB} = 15.0$ mm, respectively.

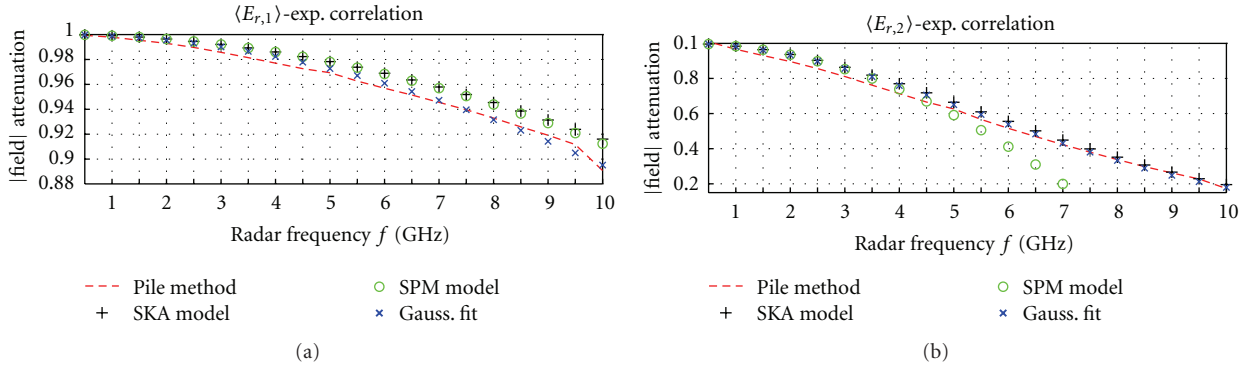

FIGURE 5: The Same simulation parameters as in Figure 4 (with $L_{cA} = 6.4$ mm and $L_{cB} = 15.0$ mm), but for exponential correlation surfaces.

$f = 4$ GHz, $\mathrm{Ra}_{r,1} = 0.084$, whereas $\mathrm{Ra}_{r,2} = 0.362$. By using a least square method on the PILE results, a Gaussian fit is also applied as a test for comparison. This fitting process confirms that the PILE method for describing the attenuation of the coherent field amplitude can be approximated by a Gaussian attenuation with respect to the frequency; the agreement is particularly good for the second-order $\langle E_{r,2}\rangle$.

Figure 3 presents the numerical results for the same parameters as in Figure 2, but for surfaces with exponential correlation. The same general comments and conclusions as for Gaussian correlation can be made here. Indeed, the results of the PILE code do not change significantly from Gaussian to exponential correlation: there is only a slight decrease for the higher frequencies here. Then, both the SKA and SPM2 models show a good agreement for $\langle E_{r,1}\rangle$, and the SKA model shows a very good agreement for $\langle E_{r,2}\rangle$. Then, it is interesting to notice that the agreement is even better for the second-order contribution, which validates the proposed approach for random rough layers. These results lead us to the conclusion that for this typical configuration, the coherent scattering of random rough layers does not change significantly from Gaussian to exponential correlation, as predicted by the SKA and SPM2 models.

For studying the validity domain of extended SKA and SPM2 models, another set of simulations is led for a different configuration. We chose to reduce the correlation length of both surfaces L_{cA} and L_{cB}: we took $L_{cA} = 6.4$ mm and $L_{cB} = 15.0$ mm and kept other parameters constant (in particular, the surface RMS heights), in order to increase the surface slopes. Indeed, as the SPM2 model is valid for small surface slopes and the SKA model is valid for negligible slopes, increasing the RMS slopes should degrade the agreement. Then, as both the SKA and SPM2 models do not depend on the surface correlation length, their results do not change with the configuration.

Associated results for Gaussian correlation can be found in Figure 4. Let us note that for Gaussian surfaces, this modification implies changing the surfaces RMS slopes from $\sigma_{sA} = 0.141$ and $\sigma_{sB} = 0.094$ to $\sigma_{sA} = 0.221$ and $\sigma_{sB} = 0.189$. Compared to Figure 2, it can be noted that the results of the PILE method slightly decrease for the first echo $\langle E_{r,1}\rangle$, and that this decrease gets stronger as the frequency increases. This decrease may be attributed to the increase of the surface slopes, which induces a broadening of the scattered field in regions away from the specular direction, which in consequence may decrease the coherent specular scattered field. Besides, despite the decrease of the PILE results, both SKA and SPM2 models show a general good agreement with the PILE method, and in particular for the lower frequencies. For the second echo $\langle E_{r,2}\rangle$, the PILE results do not change significantly: there is a slight decrease for the lower frequencies, but a slight increase for the higher

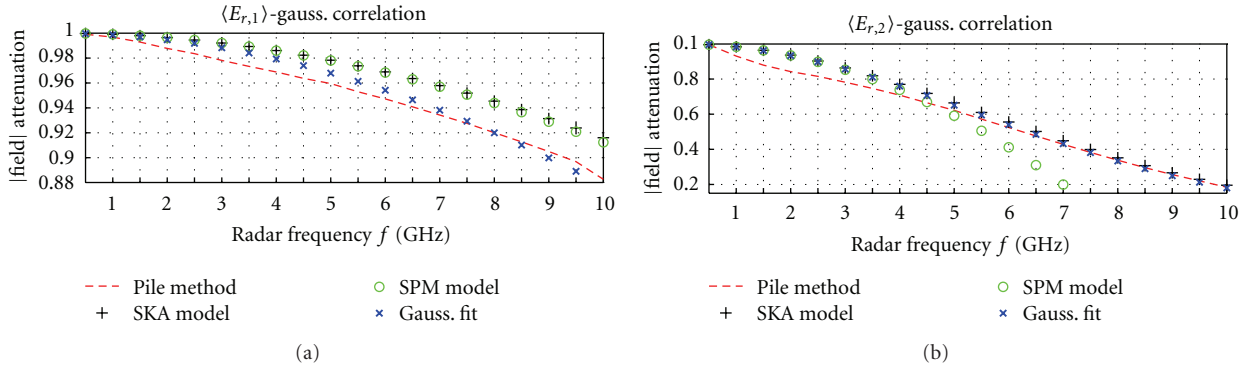

FIGURE 6: Frequency behavior of the amplitude attenuation of the coherent scattered fields $\langle E_{r,1}\rangle$ and $\langle E_{r,2}\rangle$ (V polarization) in the frequency band $f \in [0.5; 10.0]$ GHz, comparatively to the flat case: results from the PILE code and comparison with the SKA and SPM2 asymptotic models for Gaussian surfaces. The upper and lower correlation lengths are $L_{cA} = 4.0$ mm and $L_{cB} = 8.0$ mm, respectively.

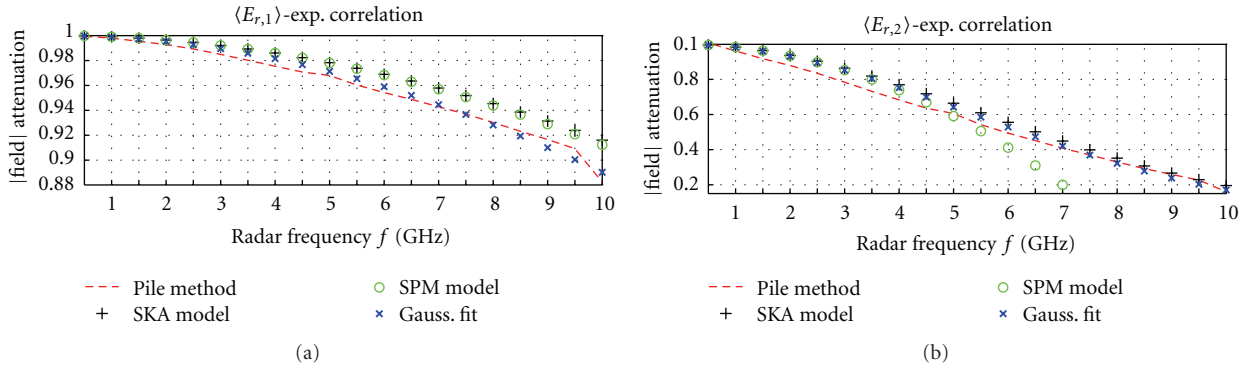

FIGURE 7: The same simulation parameters as in Figure 6 (with $L_{cA} = 4.0$ mm and $L_{cB} = 8.0$ mm), but for exponential correlation surfaces.

frequencies. Then, the SKA model remains in a very good agreement with the PILE method.

The same analysis is made on surfaces with exponential correlation in Figure 5. Similar comments can be made here by comparing Figure 5 with Figure 2: for the first echo, the PILE code slightly decreases, and this decrease gets stronger as f increases. Then, for exponential correlation here, the difference of both the SKA and SPM2 models with the PILE method begins to be rather significant for the higher frequencies, and in particular for f tending to 10 GHz. For the second echo, there is also a slight decrease of the PILE code for the lower frequencies. Thus, the SKA model remains in a (very) good agreement with the PILE method in the whole frequency range, even for the higher frequencies where the coherent attenuation is significant.

At last, 2 more sets of simulations for both Gaussian and exponential surfaces are studied: first, by increasing again the correlation lengths ($L_{cA} = 4.0$ mm and $L_{cB} = 8.0$ mm) in Figures 6 and 7 and second, by increasing the RMS heights ($\sigma_{hA} = 1.5$ mm and $\sigma_{hB} = 3.0$ mm) and correlation lengths kept constant ($L_{cA} = 6.4$ mm and $L_{cB} = 15.0$ mm) in Figures 8 and 9. First, by decreasing again the correlation lengths, as expected the agreement of both SKA and SPM models is poorer in general, and in particular for the first-order $|\langle E_{r,1}\rangle|$. The overestimation by both SKA and SPM models increases as the frequency increases (the SPM model gives slightly better agreements) and becomes significant for the higher frequencies. This is not surprising, as here the RMS slopes are significant: $\sigma_{sA} = \sigma_{sB} = 0.354$. Besides, the agreement is better for exponential correlation than for Gaussian correlation. For the second-order $|\langle E_{r,2}\rangle|$, for both correlations, slight differences occur in the range 1–4 GHz, owing to the increase of the RMS slopes ($\sigma_{sA} = \sigma_{sB} = 0.354$ here). However, the SKA model shows a general good agreement in the whole frequency range.

Second, this time (Figures 8 and 9) by increasing the RMS heights with correlation lengths kept constant ($L_{cA} = 6.4$ mm and $L_{cB} = 15.0$ mm) compared to Figures 4 and 5, the results are similar to the reference configuration ($\sigma_{hA} = 1.0$ mm and $\sigma_{hB} = 2.0$ mm). Here, this corresponds to RMS slopes $\sigma_{sA} = 0.331$ and $\sigma_{sB} = 0.283$. The main observable differences occur in the second-order $|\langle E_{r,2}\rangle|$ where the SKA model slightly overestimates the reference method for the lower frequencies, like in Figures 6 and 7. Nevertheless, here the agreement is better, and in particular for the first-order $|\langle E_{r,1}\rangle|$.

As a consequence, it can be concluded that the agreement is less sensitive to the RMS heights than the correlation lengths. The main difference is in the frequency validity domain of the SPM model: as predicted by theory, it decreases as the RMS heights increases (see in particular $|\langle E_{r,2}\rangle|$). Thus, the SKA model is in a general (very) good

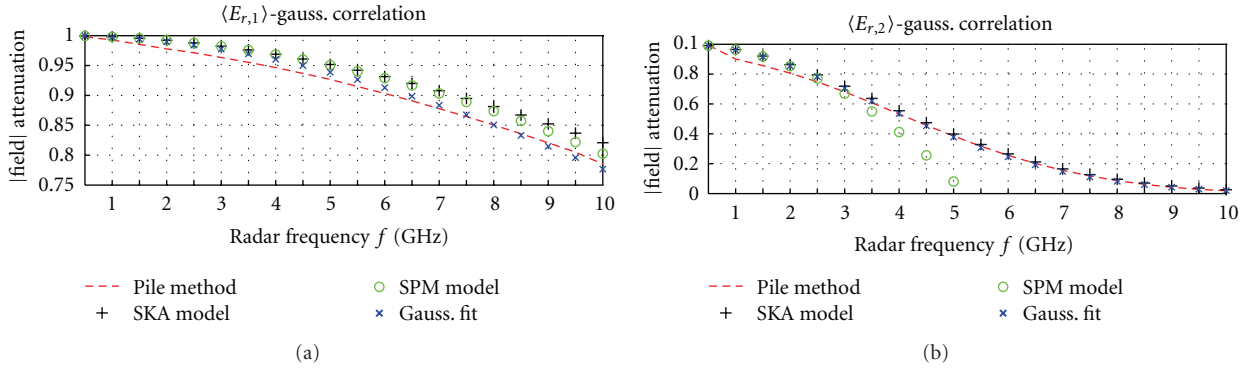

FIGURE 8: Frequency behavior of the amplitude attenuation of the coherent scattered fields $\langle E_{r,1}\rangle$ and $\langle E_{r,2}\rangle$ (V polarization) in the frequency band $f \in [0.5; 10.0]$ GHz, comparatively to the flat case. Results from the PILE code and comparison with the SKA and SPM2 asymptotic models for Gaussian surfaces. The upper and lower correlation lengths are $L_{cA} = 6.4$ mm and $L_{cB} = 15.0$ mm, respectively, and the upper and lower RMS heights are $\sigma_{hA} = 1.5$ mm and $\sigma_{hB} = 3.0$ mm, respectively.

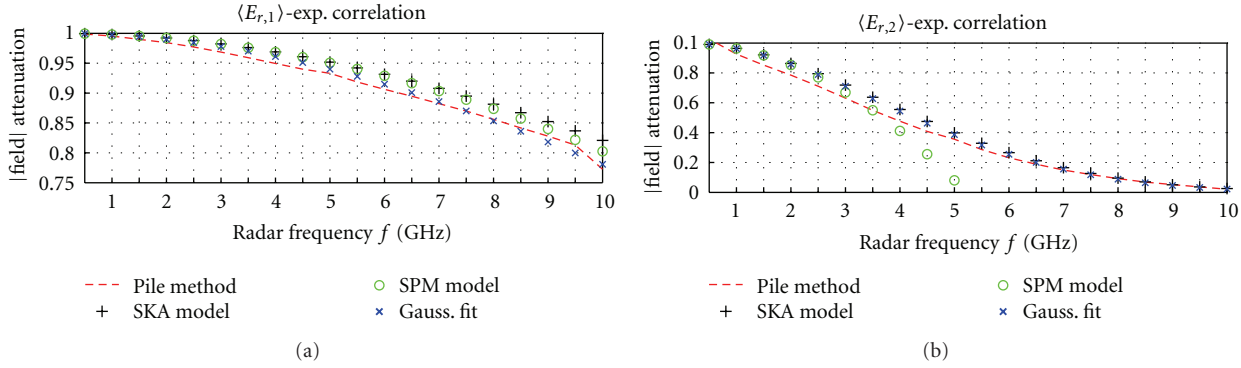

FIGURE 9: The same simulation parameters as in Figure 8 ($L_{cA} = 6.4$ mm and $L_{cB} = 15.0$ mm and $\sigma_{hA} = 1.5$ mm and $\sigma_{hB} = 3.0$ mm), but for exponential correlation surfaces.

agreement with the PILE method in the whole frequency range for both Gaussian and exponential correlations. Its main limitations are the small correlation lengths in the higher frequencies for the first-order scattered field $|\langle E_{r,1}\rangle|$.

4. Conclusion

This paper presented the extension of both the SKA and SPM2 models to coherent scattering from random rough layers, where the two random rough surfaces are uncorrelated. An application is then presented for dealing with the pavement survey by GPR at nadir, in a large frequency range ($f \in [0.5; 10.0]$ GHz), and for surfaces with both Gaussian and exponential correlations. The comparisons with a numerical reference method made it possible to validate both asymptotic models in their validity domains for 2D problems. For 3D problems, similar results and conclusions are expected, as the SKA model for describing the attenuation of the coherent scattering owing to the surface roughness is the same for 2D and 3D problems.

In particular, the SKA model was shown to correctly predict the coherent scattered field for typical configurations in pavement survey by GPR at nadir. By taking into account the time delay of each echoes in this new model, this direct simple EM model can be a good candidate for its use in signal processing algorithms for the estimation of physical parameters of the pavement like its thickness H [13, 14] and also and more important, for the estimation of the RMS heights of the rough surfaces σ_{hA} and σ_{hB} simultaneously.

References

[1] O. Landron, M. J. Feuerstein, and T. S. Rappaport, "A comparison of theoretical and empirical reflection coefficients for typical exterior wall surfaces in a mobile radio environment," *IEEE Transactions on Antennas and Propagation*, vol. 44, no. 3, pp. 341–351, 1996.

[2] D. Didascalou, M. Döttling, N. Geng, and W. Wiesbeck, "An approach to include stochastic rough surface scattering into deterministic ray-optical wave propagation modeling," *IEEE Transactions on Antennas and Propagation*, vol. 51, no. 7, pp. 1508–1515, 2003.

[3] Y. Cocheril and R. Vauzelle, "A new ray-tracing based wave propagation model including rough surfaces scattering," *Progress in Electromagnetics Research*, vol. 75, pp. 357–381, 2007.

[4] Z. Yin, Z. Akkerman, B. X. Yang, and F. W. Smith, "Optical properties and microstructure of CVD diamond films," *Diamond and Related Materials*, vol. 6, no. 1, pp. 153–158, 1997.

[5] I. Ohlídal and K. Navrátil, "Scattering of light from multilayer with rough boundaries," in *Progress in Optics*, E. Wolf, Ed., pp. 248–331, Elsevier, New York, NY, USA, 1995.

[6] A. Aziz, W. Papousek, and G. Leising, "Polychromatic reflectance and transmittance of a slab with a randomly rough boundary," *Applied Optics*, vol. 38, no. 25, pp. 5422–5428, 1999.

[7] B. Baumeier, T. A. Leskova, and A. A. Maradudin, "Transmission of light through a thin metal film with periodically and randomly corrugated surfaces," *Journal of Optics A*, vol. 8, no. 4, pp. S191–S207, 2006.

[8] T. A. Leskova and A. A. Maradudin, "Reduced Rayleigh equations in the scattering of s-polarized light from and its transmission through a film with two one-dimensional rough surfaces," in *The International Society for Optical Engineering*, Proceedings of SPIE, pp. 706505-1–706505-12, Society of Photo-Optical Instrumentation Engineers, August 2008.

[9] Z. Remes, A. Kromka, and M. Vanecek, "Towards optical-quality nanocrystalline diamond with reduced non-diamond content," *Physica Status Solidi A*, vol. 206, no. 9, pp. 2004–2008, 2009.

[10] D. E. Freund, N. E. Woods, H. C. Ku, and R. S. Awadallah, "Forward radar propagation over a rough sea surface: a numerical assessment of the Miller-Brown approximation using a horizontally polarized 3-GHz line source," *IEEE Transactions on Antennas and Propagation*, vol. 54, no. 4, pp. 1292–1304, 2006.

[11] N. Pinel, C. Bourlier, and J. Saillard, "Forward radar propagation over oil slicks on sea surfaces using the ament model with shadowing effect," *Progress in Electromagnetics Research*, vol. 76, pp. 95–126, 2007.

[12] J. S. Lee, C. Nguyen, and T. Scullion, "A novel, compact, low-cost, impulse ground-penetrating radar for nondestructive evaluation of pavements," *IEEE Transactions on Instrumentation and Measurement*, vol. 53, no. 6, pp. 1502–1509, 2004.

[13] C. L. Bastard, V. Baltazart, Y. Wang, and J. Saillard, "Thin-pavement thickness estimation using GPR with high-resolution and superresolution methods," *IEEE Transactions on Geoscience and Remote Sensing*, vol. 45, no. 8, pp. 2511–2519, 2007.

[14] N. Pinel, C. L. Bastard, V. Baltazart, C. Bourlier, and Y. Wang, "Influence of layer roughness for road survey by ground penetrating radar at nadir: theoretical study," *IET Radar, Sonar and Navigation*, vol. 5, no. 6, pp. 650–656, 2011.

[15] N. Déchamps, N. de Beaucoudrey, C. Bourlier, and S. Toutain, "Fast numerical method for electromagnetic scattering by rough layered interfaces: propagation-inside-layer expansion method," *Journal of the Optical Society of America A*, vol. 23, no. 2, pp. 359–369, 2006.

[16] J. Ogilvy, *Theory of Wave Scattering from Random Surfaces*, Institute of Physics Publishing, Bristol, UK, 1991.

[17] N. Pinel, C. Bourlier, and J. Saillard, "Degree of roughness of rough layers: extensions of the rayleigh roughness criterion and some applications," *Progress In Electromagnetics Research B*, vol. 19, pp. 41–63, 2009.

[18] Z. Yin, H. S. Tan, and F. W. Smith, "Determination of the optical constants of diamond films with a rough growth surface," *Diamond and Related Materials*, vol. 5, no. 12, pp. 1490–1496, 1996.

[19] N. Pinel and C. Bourlier, "Scattering from very rough layers under the geometric optics approximation: further investigation," *Journal of the Optical Society of America A*, vol. 25, no. 6, pp. 1293–1306, 2008.

[20] D. Franta and I. Ohlídal, "Comparison of effective medium approximation and Rayleigh-Rice theory concerning ellipsometric characterization of rough surfaces," *Optics Communications*, vol. 248, no. 4–6, pp. 459–467, 2005.

[21] N. Dechamps and C. Bourlier, "Electromagnetic scattering from a rough layer: propagation-inside-layer expansion method combined to an updated BMIA/CAG approach," *IEEE Transactions on Antennas and Propagation*, vol. 55, no. 10, pp. 2790–2802, 2007.

[22] N. Déchamps and C. Bourlier, "Electromagnetic scattering from a rough layer: propagation-inside-layer expansion method combined to the forward-backward novel spectral acceleration," *IEEE Transactions on Antennas and Propagation*, vol. 55, no. 12, pp. 3576–3586, 2007.

[23] A. Iodice, "Forward-backward method for scattering from dielectric rough surfaces," *IEEE Transactions on Antennas and Propagation*, vol. 50, no. 7, pp. 901–911, 2002.

[24] H. T. Chou and J. T. Johnson, "A novel acceleration algorithm for the computation of scattering from rough surfaces with the forward-backward method," *Radio Science*, vol. 33, no. 5, pp. 1277–1287, 1998.

[25] H. T. Chou and J. T. Johnson, "Formulation of forward-backward method using novel spectral acceleration for the modeling of scattering from impedance rough surfaces," *IEEE Transactions on Geoscience and Remote Sensing*, vol. 38, no. 1, pp. 605–607, 2000.

[26] C. D. Moss, T. M. Grzegorczyk, H. C. Han, and J. A. Kong, "Forward-backward method with spectral acceleration for scattering from layered rough surfaces," *IEEE Transactions on Antennas and Propagation*, vol. 54, no. 3, pp. 1006–1016, 2006.

[27] R. Wu, X. Li, and J. Li, "Continuous pavement profiling with groundpenetrating radar," *Radar, Sonar and Navigation*, vol. 149, pp. 183–193, 2002.

[28] "AFNOR standard NFP 98-137," French standard, 1992.

[29] K. Sarabandi, E. S. Li, and A. Nashashibi, "Modeling and measurements of scattering from road surfaces at millimeter-wave frequencies," *IEEE Transactions on Antennas and Propagation*, vol. 45, no. 11, pp. 1679–1688, 1997.

[30] F. Koudogbo, H. J. Mametsa, and P. F. Combes, "Surface and volume scattering from natural and manmade rough surfaces in the process of setting up data base coefficients," in *Proceedings of the IEEE International Geoscience and Remote Sensing Symposium*, vol. 7, pp. 4211–4213, Piscataway, NJ, USA, July 2003.

[31] M. Adous, P. Quéffélec, and L. Laguerre, "Coaxial/cylindrical transition line for broadband permittivity measurement of civil engineering materials," *Measurement Science and Technology*, vol. 17, no. 8, pp. 2241–2246, 2006.

[32] C. Fauchard, *Utilisation de Radars trés hautes fréquences : application á l'uscultation non destructive des chaussées [Ph.D. thesis]*, University of Nantes, Nantes, France, 2001.

[33] E. S. Li and K. Sarabandi, "Low grazing incidence millimeter-wave scattering models and measurements for various road surfaces," *IEEE Transactions on Antennas and Propagation*, vol. 47, no. 5, pp. 851–861, 1999.

[34] F. Koudogbo, P. Combes, and H. J. Mametsa, "Numerical and experimental made rough surfaces," *Progress in Electromagnetics Research*, vol. 46, pp. 203–244, 2004.

[35] S. Lambot, E. C. Slob, I. van den Bosch, B. Stockbroeckx, and M. Vanclooster, "Modeling of ground-penetrating radar for accurate characterization of subsurface electric properties," *IEEE Transactions on Geoscience and Remote Sensing*, vol. 42, no. 11, pp. 2555–2568, 2004.

[36] F. Liu, *Modélisation et Expérimentation Radar Impulsionnel et á Sauts de Fréquence Pour l'Auscultation de Milieux Stratifiés du Génie Civil [Ph.D. thesis]*, University of Nantes, Nantes, France, 2007.

[37] E. Thorsos and D. Jackson, "Studies of scattering theory using numerical methods," *Waves in Random Media*, vol. 1, pp. 165–190, 1991.